Title

THE LOWEST TRIPLET STATE OP SUBSTITUTED BENZENES: III. OPTICALLY DETECTED MAGNETIC RESONANCE STUDIES ON THE 3nn* STATE OF l,2,4,5-TETRABROMOBENZENE AND 1,2,4,5-TETRACHLOROBENZENE

Author

Francis, A.H.

Publication Date

1972

Submitted to Journal of
Chemical Physics

LBL-472
Preprint

THE LOWEST TRIPLET STATE OF SUBSTITUTED BENZENES: III. OPTICALLY DETECTED MAGNETIC RESONANCE STUDIES ON THE $^3\pi\pi^*$ STATE OF 1,2,4,5-TETRABROMOBENZENE AND 1,2,4,5-TETRACHLOROBENZENE

A. H. Francis and C. B. Harris

January 1972

AEC Contract No. W-7405-eng-48

DISCLAIMER

UNIVERSITY OF CALIFORNIA

Lawrence Berkeley Laboratory

Berkeley, California

April 14, 1972

ERRATA

To: All recipients of LBL 472.

From: Inorganic Materials Research Division and Technical Information Division

Subject: LBL-472, "The Lowest Triplet State of Substituted Benzenes: III. Optically Detected Magnetic Resonance Studies on the $^3\pi\pi^*$ State of 1,2,4,5-Tetrabromobenzene and 1,2,4,5-Tetrachlorobenzene, by A. H. Francis and C. B. Harris, dated January 1972.

Please add Acknowledgements page to subject report.

VI. ACKNOWLEDGEMENTS

This work was supported by the Inorganic Materials Research Division of the Lawrence Berkeley Laboratory under the auspices of the U. S. Atomic Energy Commission. The authors would like to acknowledge the assistance of Dr. Steven Gaudioso, (Department of Chemistry, University of Michigan, Ann Arbor, Michigan), who supplied the Raman spectra of TBB.

The Lowest Triplet State of Substituted Benzenes: III. Optically Detected Magnetic Resonance Studies on the $^3\pi\pi^*$ State of 1,2,4,5-tetrabromobenzene and 1,2,4,5-tetrachlorobenzene.

by

A. H. Francis[†] and C. B. Harris[‡]

Department of Chemistry, University of California, and
Inorganic Materials Research Division, Lawrence Berkeley Laboratory
Berkeley, California 94720

ABSTRACT

The optically detected magnetic resonance (ODMR) in zero field and the phosphorescence microwave double resonance (PMDR) spectra of 1,2,4,5-tetrabromobenzene and 1,2,4,5-tetrachlorobenzene have been obtained monitoring the low temperature (1.3°K) phosphorescence from both trap emission in neat single crystals and emission from a durene host. From the PMDR the major vibronic features of the spectra are assigned. The orbital symmetries in the excited triplet state, the principal and secondary contributions from the individual triplet spin sublevels to the electronic and vibronic origins in phosphorescence, the spin sublevel populations and lifetimes are determined. In addition the spin

---

[†] Present address: Department of Chemistry, University of Illinois at Chicago Circle, Chicago, Illinois 60680

[‡] Alfred P. Sloan Fellow; to whom correspondence should be addressed.

Hamiltonian parameters including the zero-field splittings, Br and Cl excited state nuclear quadrupole coupling constants are presented and interpreted. Finally, the relationship between spin sublevel activity in phosphorescence, Franck-Condon maxima in emission and molecular distortions are discussed.

I. INTRODUCTION

A considerable amount of information has been generated by spectroscopist and theorist alike concerning the properties of planar aromatics and azaaromatics in excited triplet states. Early investigations centered around benzene, dealing principally with the classification of the orbital symmetry of the lowest triplet state. Although there was some disagreement among experimentalists[1] as to the state that gives rise to the weak phosphorescence activity, most theorists[2] generally agreed that in benzene the lowest excited state was $^3B_{1u}$. Similar disagreement exists among spectroscopists about the lowest triplet states and excited state geometry in halogenated benzenes.[3,4] Although the possible routes by which electric dipole allowed character can be mixed into the triplet spin sublevels were elucidated by Albrecht,[5] experimental confirmation of the triplet orbital symmetry in benzene and substituted benzenes has not, until recently, been generally possible. To unambiguously assign the triplet orbital symmetry requires a knowledge of the magnetic orientations and spin-orbit symmetries of the triplet spin sublevels. Since the zeroth order wavefunctions for each triplet spin sublevel transform as the direct product of the irreducible representations of spatial and spin functions, knowledge of either the spin-orbit symmetry of all three spin sublevels or both the magnetic orientation and spin-orbit symmetry of one sublevel is required for an orbital assignment. A technique which has recently been developed to provide the necessary information about the triplet spin sublevels is optically detected magnetic resonance (ODMR).[6] In addition to providing parameters associated with the electron distribution in excited states such as the

zero-field splittings, the electron-nuclear hyperfine and the nuclear quadrupole coupling constants, it has been utilized to determine the rates and routes of intramolecular energy transfer.[7,8,9] In this manner not only can the symmetries of the individual spin sublevels be determined but the relative importance of the specific routes by which dipole activity is mixed into the triplet spin sublevels can be assessed. The techniques have been applied quantitatively principally by van der Waals and Schmidt,[10] Ed-Sayed[8] and by Harris[11,12] and co-workers using optical detection, and by Schwoerer and Sixl[13] using conventional ESR techniques.

As part of a general investigation of the properties of the lowest excited triplet state of halogenated benzenes, considerable progress has been achieved in characterizing the electron distribution and the orbital symmetry, and elucidating the radiative routes for electronic relaxation. In the first two papers[12,14] in this series paradichlorobenzene was extensively studied. In the following, the tetrahalobenzenes are investigated. Specifically the results of phosphorescence microwave double resonance (PMDR) studies[15] obtained for 1,2,4,5-tetrabromobenzene (TBB) and 1,2,4,5-tetrachlorobenzene (TCB) neat and doped in a durene host are presented.

II. EXPERIMENTAL

A. Sample Preparation

TCB and TBB were purified by extensive zone refining (200 passes at approximately 1 cm/hour). A single crystal of the β phase of TCB was prepared from the zone-refined material by standard Bridgeman techniques. The β phase is monoclinic $P2_1/a$ (C_{2h}^5);[16] however below 188°K TCB converts to a triclinic $P\bar{1}$ α phase with two molecules per unit cell.[17,18,19] The presence of a high temperature phase transition in TBB prevented preparation of single crystals by Bridgeman methods. The crystals tend to shatter as they pass through the phase transition. The material initially crystallized in its γ phase, monoclinic $P2_1/a$ (C_{2h}^5) with two molecules per unit cell.[20] Single crystals of the β phase could be obtained from CS_2 solution as platelets elongated along the c crystallographic axis showing (110) faces.[18]

TCB and TBB were also studied in a durene host lattice. Mixed crystals of approximately 1% m/m were prepared by the Bridgeman method using commercially available zone-refined durene supplied by Eastman. The doped durene crystals were cut parallel to the (010) plane and the crystal orientations were determined coniscopically and verified by x-ray diffraction using the precession method. The single crystals were mounted in the appropriate orientation inside a slow wave microwave helix affixed to a section of rigid 50 Ω coaxial cable. The entire assembly was suspended in a liquid He dewar which could be pumped to a temperature of 1.3°K. The crystals were slowly (~ 2 hr) cooled to 77°K to prevent cracking from thermal shock.

The phosphorescence spectra were obtained by placing the exciting source, a 3/4 meter Jarrell-Ash scanning monochrometer equipped with an EMI 9856-QB thermoelectrically cooled photomultiplier and sample in a 90° configuration. All phosphorescence spectra and PMDR spectra were obtained using as an exciting source the 3100 Å region of a PEK 100 watt Xe-Hg high pressure short arc. The absorption spectra of TBB were obtained by passing a Xe continuum (75 watt PEK Xe lamp) through a pin hole in an aluminum plate over which a single crystal was mounted.

B. Optically Detected Magnetic Resonance and PMDR Spectra

The zero-field optically detected magnetic resonance (ODMR) of TCB and TBB were obtained monitoring the unpolarized phosphorescence from the appropriate crystals at 1.3°K. The microwaves were supplied by a Hewlett-Packard sweep generator, amplified by a 20 watt TWT and terminated in the 50 Ω coaxial line. The microwaves were amplitude modulated at 5 Hz/sec with a pin modulator at a modulation depth greater than 30 db. The output of the photomultiplier was phase detected using a PAR HR-8 lock-in amplifier. Other details of the experimental arrangement are essentially those reported by Buckley and Harris.[14]

The unpolarized PMDR spectra were obtained in a manner similar to those reported earlier for paradichlorobenzene.[12,14] The polarized PMDR spectra[21] in TBB doped in durene were obtained while monitoring emission from the appropriate crystallographic face and separating the polarized components with fused silica discs coated with polacoat 105 uv. All spectra were obtained amplitude modulating the appropriate zero-field

microwave transitions at 25 Hz/sec and using phase detection techniques while scanning the phosphorescence spectrum at 25 Å/min.

C. Adiabatic Inversion

The adiabatic inversion[9] of the populations remaining in the spin sublevels after the exciting source has been removed was conducted at 1.3°K employing the same procedure for adiabatic fast passage as reported by Harris and Hoover.[22] An optimum inversion of 85% of the sublevel populations could be achieved with a sweep rate of 10 MHz/80 μsec and microwave power incident on the sample of 0.03 gauss. Using the inversion technique the lifetimes of all three spin sublevels for both TBB and TCB were measured in a manner similar to that reported by Schmidt, Veeman and van der Waals.[7] In addition the relative radiative rate constants for the y-trap phosphorescence in the electronic origin and the b_{2g} vibronic origin were obtained for TCB. These data are summarized in Table V.

III. RESULTS

The unpolarized (high resolution), ||a and ||c' polarized (medium resolution) single crystal phosphorescence spectrum for TBB doped in durene is illustrated in Fig. 1 while the wavelengths, polarization ratios and assignments are tabulated in Table I. The optically detected zero-field microwave transitions for TBB in durene and neat TBB are listed in Table II in terms of the conventional zero-field parameters D and E. Included in Table II are the values for TCB. The 2|E| and D-|E| optically detected zero-field transitions in TBB doped in durene were obtained monitoring the phosphorescence electronic origin and are illustrated in Fig. 2. The D+|E| transition (not shown) is essentially the same. The spectra consisted of a center peak flanked by three pairs of satellites separated from the main central peak by 277, 230, and 47 MHz respectively. These satellites result from nuclear hyperfine and nuclear quadrupole coupling of the bromine nuclei in the excited triplet state. The details of these transitions will be discussed in a later section. The unpolarized, the ||a polarized and the ||c' polarized PMDR spectra of TBB in durene are each illustrated in Figures 3-5 for the D+|E|, D-|E| and 2|E| zero-field transitions respectively. The unpolarized single crystal phosphorescence spectrum of neat TBB at 4.2°K is illustrated in Fig. 6. The single crystal absorption spectrum of neat TBB (bc face)' is illustrated in Fig. 7a, while the ||c' and ||b polarized absorption spectra in the electronic origin are illustrated in Fig. 7b and 7c respectively. These spectra were obtained at 1.35°K. The

wavelengths corresponding to the major features of the absorption spectra are tabulated in Table III while the room temperature Raman frequencies are listed in Table IV along with their assignments. All transitions in Fig. 7a were found to have about the same (± 10%) polarization ratios as the electronic origin. The data illustrated in Fig. 7 were obtained from a single crystal 0.5 mm thick.

The optically detected zero-field microwave transitions in neat TCB for x-trap, y-trap and exciton emission have been reported earlier by Francis and Harris,[23] while the details of the phosphorescence spectra have been reported and discussed by George and Morris.[24] The zero-field transitions and phosphorescence spectra reported for TCB doped in durene[25] are essentially the same as those reported for neat TCB.[23,24] The PMDR spectra for TCB (neat and doped in durene) and neat TBB are not illustrated;[26] however, the pertinent information for the electronic origin, b_{1g} and b_{2g} vibronic origins are listed in Table V. This data includes the optical frequencies, the direction and relative intensity in the PMDR transitions. Included in Table V are the relative radiative rate constants from the individual spin sublevels and the total decay constants (1/e values) for the three zero-field sublevels τ_x, τ_y and τ_z as obtained from the decay-inversion experiments outlined above.

IV. DISCUSSION

In the following discussion we will use the convention suggested by Mulliken[27] for the directions associated with the molecular axes. Both in TBB and TCB the z axis is defined along the C-H bonds, the y axis as in-plane along the halogen bisector and the x axis as normal to the molecular plane. In this axis system the vectors X, Y and Z transform respectively as B_{3u}, B_{2u} and B_{1u} irreducible representations of the D_{2h} molecular point group and rotations around these axes transform as B_{3g}, B_{2g} and B_{1g}.

A. Interpretation of the PMDR Spectra and Vibronic Analysis of TBB in Durene

The polarized PMDR spectra illustrated in Figures 3-5 allow one to determine which spin sublevels are primarily responsible for the intensity of a particular phosphorescence transition. Consider first the phosphorescence electronic origin. It is apparent from the data that its principal electric dipole activity is from a single spin sublevel, τ_i, which is common to both the $2|E|$ and $D+|E|$ zero-field microwave transitions. Assuming that the spin sublevel primarily responsible for the electric dipole activity of electronic origin is the same in the neat crystal as in durene host[28] and utilizing polarization results in the single crystal $T_1 \leftarrow S_0$ absorption spectrum in Fig. 7 we can conclusively assign out-of-plane (x) polarization from τ_i. This requires its spin-orbit symmetry to be B_{3u}. The PMDR data also show that there

is negligible dipole activity in the electronic origin from the middle spin sublevel τ_{ii} and that the third spin sublevel, τ_{iii}, which is common to both the D-|E| and D+|E| transitions shows a small but finite contribution to the electronic origin. In addition the spin sublevel (τ_{iii}) responsible for the minor route in origin phosphorescence must have the largest steady state population under CW excitation since the origin phosphorescence intensity increases when the 2|E| and D+|E| transitions are pumped and decreases when the D-|E| transition is pumped. The (0,-208 cm^{-1}) transition, however, shows an increase in both the D+|E| and D-|E| PMDR spectra. From the above, τ_i is established as having the smallest population at steady state and the populations must be ordered $N_i < N_{ii} < N_{iii}$ for TBB doped in durene.

The polarization ratios in the D+|E| and D-|E| polarized PMDR's clearly indicate the lack of z polarized phosphorescence from τ_{iii} to the electronic origin; consequently the spin-orbit symmetry of τ_{iii} can be assigned as B_{2u} since B_{3u} has been shown to be associated with τ_i. Naturally this assumes that durene is isomorphously replaced by TBB in the host. The high polarization ratios obtained are consistent with this view and allow the separation of the z component from the x and y components in the durene crystallographic space group.[28]

The remaining spin sublevel, τ_{ii}, may have an overall spin-orbit symmetry of either B_{1u} or A_u. By analogy to benzene and substituted benzenes, in which the lowest triplet state is believed to be $^3B_{1u}$, τ_{ii} would be expected to have A_u spin-orbit symmetry. A spin-orbit symmetry of B_{1u} for τ_{ii} would require the orbital symmetry of the

emitting triplet to the ^3A_u. No assumptions need be made, however, since examinations of the polarized PMDR spectra can uniquely establish τ_{ii} as A_u.

The lack of any emission to the electronic origin from τ_{ii} is consistent with an A_u spin-orbit state, which is electric dipole forbidden in the D_{2h} molecular point group. The site symmetry, assuming isomorphic replacement of TBB in durene, is C_i. In this point group the transition from the τ_{ii} (A_u) spin sublevel to the origin becomes formally allowed; however, the absence of emission suggests that the durene host has little effect on the molecular symmetry of TBB.

The strongest evidence for the A_u assignment of τ_{ii} is obtained from the vibronic analysis of the PMDR spectra. The electric dipole activity of the (0,-208 cm^{-1}) vibration can be established from the PMDR spectra illustrated in Figs. 3-5 as arising primarily from τ_{ii} with x and/or y polarization and secondarily from τ_i with z polarization exclusively, consistent with emission to a b_{2g} vibration. This assignment is also consistent with the Raman data. Because of favorable direction cosines in durene,[28] the single b_{1g} vibrations can be easily identified in the polarized emission spectra. The b_{1g} fundamental and the overall b_{1g} combination bands (0,-995 cm^{-1}, 0,-1447 cm^{-1}) all show an a/c' polarization ratio less than unity, while all other bands show ratios greater than unity. We assign the b_{1g} fundamental in the durene host as (0,-325 cm^{-1}) in agreement with the Raman data. The large increase in the D-|E| polarized PMDR parallel to z indicates that the largest contribution to the emission intensity is from the A_u state, τ_{ii}. This

is further supported by the decrease in the z polarized 2|E| PMDR. The small increase in activity in the x and/or y polarization is consistent with a minor contribution from the τ_i level with y polarization. No activity can be attributed to either the b_{1g} or b_{2g} vibration from the τ_{iii} spin sublevel.

From the above analysis we can assign the spin-orbit symmetry of all spin sublevels. They are τ_i: B_{3u}; τ_{ii}: A_u; and τ_{iii}: B_{2u}. These correspond to the spin sublevel spin-orbit symmetries of a $^3B_{1u}$ state. The $^3B_{1u}$ assignment of the lowest triplet in TBB establishes that the spin sublevels $\tau_i = \tau_y$; $\tau_{ii} = \tau_z$; and $\tau_{iii} = \tau_x$.

The complete vibronic analysis of an emission spectrum based solely upon polarization data is, at best, difficult and often impossible in view of depolarization effects commonly observed in emission. The power of the PMDR data in simplifying this task is illustrated by the analysis in Table I. A convincing assignment of the major vibronic features of the TBB phosphorescence can be made utilizing a PMDR code which reflects the populations and relative radiative rate constants of the individual magnetic sublevels. The signs +, - and o in the code indicate an increase, decrease or indeterminate change in the phosphorescence intensity when the D+|E|, D-|E| and 2|E| zero-field optically detected microwave transitions are monitored. The PMDR code is given for both polarizations for the ratio a/c'. Because all transitions of the same overall symmetry are expected to have the same code, fundamentals and binary combinations are easily identified. In fact all transitions listed in Table II have been assigned on this basis with the exception of a transition at 24,925 cm^{-1}.

B. Interpretation of the TBB Single Crystal PMDR Spectra at 1.3°K

Since the analysis of the trap phosphorescence in neat TBB crystals parallels that of TBB in a durene host, we will concentrate only on several features of particular interest. First, the similarity of the zero-field parameters and PMDR spectra of TBB in durene and in neat crystals is strong evidence that the order and spin-orbit symmetry of the zero-field spin states are the same. The order of the population in the sublevels under steady state illuminating conditions is, however, different in neat TBB and in a durene host. Using the unpolarized PMDR code obtained from neat TBB at 1.3°K listed in Table VI for the electronic origin, the b_{2g} and b_{1g} fundamentals, we find that the population in neat TBB must be ordered $N_z < N_y < N_x$. This is reflected by the increase in the origin intensity in the D+|E| zero-field transition, an increase in the b_{2g} vibronic transition in the 2|E| PMDR spectra and a decrease in the 2|E| PMDR spectra. The transitions show behavior in the 2|E| PMDR pattern opposite to that in TBB doped in a durene host. The reversal in the N_y and N_z populations in a durene host is not entirely unexpected since the host can have a direct effect on the rates of populating and depopulating the spin sublevels by, for example, heavy atom effect,[29] spin lattice relaxation,[30] or indirectly through energy migration.[31] All these phenomena are expected to influence the spin alignment of triplet states. It is for these reasons that caution must be exercised in interpreting the spin alignment exclusively in terms of molecular properties such as intersystem crossing ratios.

Finally as in durene the A_u spin sublevel remains completely inactive in the electronic origin in TBB single crystals. The reduction of the molecular symmetry (D_{2h}) to the crystal site symmetry (C_i) in TBB [17,18,19] does not seem to be an important consideration in analyzing the data. If crystal field effects were important the A_u spin sublevel (τ_z) state might be expected to gain dipole activity via the reduction of the molecular point group, particularly in view of the strong dipole activity of A_u to the b_{1g} and b_{2g} vibrations.

C. Interpretation of the PMDR Spectra and Partial Vibronic Analysis of Single Crystal TCB

The emission and excitation spectra of TCB at 4.2°K have been reported by George and Morris.[24] At 4.2°K TCB shows intrinsic exciton emission as well as emission from two distinct traps. Emission from the deeper trap (y-trap), 48 cm^{-1} below the exciton origin, can be substantially enhanced by doping with other halogenated benzenes[31] whose lowest triplet states are at higher energies. The second trap (x-trap) is 22 cm^{-1} below the exciton band and shows practically no emission at 4.2°K; however, at 1.35°K these traps are responsible for almost all the phosphorescence. The x-trap is not enhanced by the addition of chemical impurities, but shows a marked dependence on the method of crystal preparation and, accordingly, is thought to be mechanical in origin.

The zero-field transitions and spin Hamiltonian parameters for the exciton, y-trap and x-trap have been reported earlier by Francis

and Harris.[23] The results from a single crystal unpolarized PMDR spectrum at 1.3°K of TCB and the relative intensities of the respective transitions are listed in Table V. For the purposes of this discussion it will be sufficient to consider only the electronic origin (0,0), a single b_{2g} fundamental (0,-233 cm^{-1}) and the b_{1g} fundamental (0,-363 cm^{-1}).[32]

The fact that the phosphorescence to the origin increases for both the D+|E| and D-|E| microwave transitions while it decreases in the 2|E| PMDR establishes one of the following relations: (a) the spin sublevel common to the D-|E| and 2|E| transitions (τ_{ii}) is most active to the origin and the population in τ_{ii} is greater than that in τ_i (the spin sublevel common to the 2|E| and D+|E| transitions) and the populations are ordered $N_{iii} > N_{ii} > N_i$; (b) τ_i has a larger dipole activity to the origin than τ_{ii} or τ_{iii} and the populations are ordered $N_{iii} > N_i > N_{ii}$; or (c) τ_{iii}, the spin sublevel common to both the D+|E| and D-|E| zero-field transitions has the largest dipole activity to both the origin and the b_{2g} vibration and the populations are ordered $N_{iii} > N_{ii} > N_i$. The second possibility (b) can be ruled out by the fact that all three zero-field microwave transitions result in an increased phosphorescence to b_{2g} and that the largest change is associated with the D+|E| transition. If N_{iii} were greater than both N_i and N_{ii}, then at least one zero-field transition would result in a decreased b_{2g} phosphorescence or if all microwave transitions resulted in an increased b_{2g} phosphorescence, then the D-|E| transition should produce the largest change, which it did not.

In order to distinguish between possibilities (a) and (c), an experiment similar to those developed by van der Waals and co-workers[7] was performed. After removing the exciting source, the phosphorescence was allowed to decay for approximately 400 msec, at which time the remaining populations of τ_i and τ_{iii} were inverted via adiabatic fast passage through the D+|E| transition using the method of Harris and Hoover.[22] The same experiment was repeated for the D-|E| transition. In both cases the origin phosphorescence intensity increased upon inversion. Since no signal could be detected under the same conditions when fast passage through the 2|E| transition was attempted, one must conclude that τ_i and τ_{ii} have total decay rates much faster than τ_{iii} and that the steady state populations are ordered $N_{iii} > N_{ii} > N_i$.

These experiments also provide the decay constants for τ_i, τ_{ii} and τ_{iii} and the ratios of the radiative rate constants from the individual spin sublevels to the electronic origin and the b_{2g} vibration. These are listed in Table V according to the assignments made in the following discussion.

It is apparent that the spin sublevel τ_i is primarily responsible for the phosphorescence intensity in the electronic origin while τ_{ii} contributes principally to the b_{2g} vibronic origin. Although the phosphorescence decay and inversion experiments were not performed while monitoring the b_{1g} fundamental, it is apparent from the PMDR spectra that the largest phosphorescence change is observed while saturating the D+|E| transition and the smallest change while saturating the 2|E| transition. Therefore, like the b_{2g} vibration, b_{1g} is also most active

from the τ_i spin sublevel. There is no evidence of phosphorescence to the b_{2g} vibronic origin from the τ_{iii} spin sublevel in either the PMDR experiments or in the decay experiments.

An assignment of the spin-orbit symmetries of the magnetic sublevels can be made if one assumes that the lowest triplet state is $\pi\pi^*$ in character. The value of the zero-field parameter D typical of most $\pi\pi^*$ states[33] lends strong support to this assumption. Furthermore, there are no known benzene derivatives whose lowest triplet state corresponds to $n\pi^*$ (or $\sigma\pi^*$) symmetry. Assigning τ_i as A_u, τ_{ii} as B_{3u} and τ_{iii} as B_{2u} is the most consistent although the assignment of τ_{iii} is somewhat speculative since it is based only upon negative data. As will be discussed in section G, the magnitude of the zero-field parameter E is consistent with this symmetry and in fact provides complementary evidence for the assignment. The overall orbital symmetry of the triplet state, as in TBB, would appear to be $^3B_{1u}$.

D. Interpretation of the PMDR Spectra and Partial Vibronic Analysis of TCB Doped in Durene

Although a partial polarized PMDR study of TCB doped in durene has already been published,[25] no explicit vibronic analysis of the phosphorescence spectra was presented. The phosphorescence spectrum in durene, however, is practically identical to that reported by George and Morris[24] for the single crystal. Utilizing the PMDR data already published[25] in addition to the data collected in the course of the present investigation, it is possible to, as in the pure crystal study, determine the relative spin sublevel order and the relative population order.

It was found[25] that the phosphorescence intensity of the electronic origin increased in the D-|E| PMDR spectrum and increased in the 2|E|, the reverse of the single crystal behavior. No resonance signal could be observed for the D+|E| transition monitoring either the electronic origin or the b_{2g} vibronic origin. These observations are consistent with the spin-orbit symmetry assignments derived from the single crystal data with a change in the relative spin sublevel populations (vs. neat TCB) such that $N_{iii} > N_i > N_{ii}$. The fact that no PMDR under steady state conditions could be observed for the D+|E| transition strongly suggests that $N_i \simeq N_{iii}$. Table V summarizes the approximate magnitudes of the PMDR changes for the vibronic transitions under consideration.

The $\tau_{iii} \rightarrow \tau_{ii}$ microwave transition moment has been reported as z polarized; however, the method[34] used in this measurement can be subject to error because of the peculiar mode patterns of slow wave helices. It is known that the mode pattern supported by slow wave helices can result in an rf H_1 field which need not be parallel to the axis of the helix for all operating conditions.[35] Indeed, in some modes greater H_1 fields can be supported perpendicular to the helical axes or even radially outside the helix and these variations are frequency dependent. Accordingly, the data from such experiments must be cautiously interpreted, particularly when the helix is not impedence matched to the coaxial line.

E. Spin-Orbit Coupling Mechanism

The phosphorescence spectra of TCB and TBB are similar to those of previously studied halo-derivatives of naphthalene[36] in that the spectrum may be divided into two sub-spectra, one based on the electronic origin (sub-spectrum I) and the other based on an intense b_{2g} vibronic origin involving an out-of-plane carbon-halogen bending fundamental (sub-spectrum II). Although some ambiguity exists in the identification of the fundamental responsible for the vibronically induced intensity in the naphthalene derivatives, the mode is unambiguously identified for the halo-derivatives of benzene. As in the naphthalene derivatives, the two sub-spectra are oppositely polarized; however, the vibronically induced intensity is appreciably greater than the intensity associated with the spectrum based on the electronic origin. In the derivatives of naphthalene the two sub-spectra share the total phosphorescence intensity about equally. In both cases the division of total phosphorescence intensity between the two sub-spectra is more or less insensitive to the atomic number of the halogen substituent.

If multicenter integrals are neglected, it can easily be demonstrated that direct spin-orbit coupling between states of similar orbital configuration is ineffective in planar aromatic molecules.[37] The practical consequence of this fact is that effective spin-orbit coupling of the lowest triplet $\pi\pi^*$ state involves only high energy singlet $\sigma\pi^*$ states. The $\pi\pi^*$ states possess a node in the plane of the ring and consequently, for a molecule with D_{2h} symmetry, must transform orbitally as B_{1u}, B_{2u}, A_g or B_{3g}. All $\sigma\pi^*$ states or $n\pi^*$ states in the event a heteroatom or

substituent with occupied non-bonding orbitals is present must transform as A_u, B_{3u}, B_{1g} or B_{2g}. Of these states, transitions from the totally symmetric ground state are allowed by electric dipole selection rules only to the $^1B_{3u}$, and it is for this reason that in the majority of hydrocarbons the lowest $\pi\pi^*$ state gains electric dipole activity via direct spin-orbit coupling with a $^1B_{3u}$ state.

Sub-spectra I and II are easily separated by their different $2|E|$ PMDR behavior, as shown clearly in Fig. 5b for TBB. All features which increase in intensity (except the b_{1g} vibrations and overtones) belong to sub-spectrum I, and those which decrease, to sub-spectrum II. If we confine our attention for the moment only to the electronic origin and associated totally symmetric vibronic features (i.e., sub-spectrum I) of TCB and TBB as observed both in emission and absorption and thereby eliminate spin-vibronic and vibronic-spin-orbit coupling mechanisms, the data are quite consistent with the $^3B_{1u}$ assignment. The active spin sublevel transforms as B_{3u} (τ_y) and gains electric dipole activity in both emission and absorption by direct spin-orbit coupling with a higher lying $^1B_{3u}$, $\sigma\pi^*$ or $n\pi^*$ state. Allowed singlet character admixed in this fashion is presumably distributed, according to the Franck-Condon principle, between the electronic origin and the several active totally symmetric vibrations. It is clear from the PMDR data that essentially all of the sub-spectrum I intensity is derived exclusively in this manner.

Sub-spectrum II must gain electric dipole activity via either first-order spin-vibronic or second-order vibronic-spin-orbit interaction. The first process is neglected as a small interaction. Since the vibronic

features of sub-spectrum II are in-plane y polarized, the admixed singlet states must be $^1B_{2u}$ and $\pi\pi^*$ configurationally. The importance of vibronic-spin-orbit coupling with $\pi\pi^*$ states, relative to direct spin-orbit coupling with $\sigma\pi^*$ and $n\pi^*$ states, is largely a result of the lower energy and larger electric dipole transition moment associated with $\pi\pi^*$ states involved in the former process.

A small amount of in-plane long axis (z) polarized phosphorescence induced by b_{1g} modes implies some vibronic-spin-orbit coupling to $^1B_{1u}$ ($\pi\pi^*$) states. The greater vibronic activity induced by b_{2g} modes as compared to b_{1g} modes is partially a consequence of the b_{1g} vibrational deficiency. There is only one b_{1g} fundamental and this involves, principally, a C-H out-of-plane bend, which is not expected to be effective in inducing vibronic activity. No b_{3g} fundamentals or combinations are observed in the phosphorescence spectrum of TBB or TCB. The three b_{3g} fundamentals, which involve in-plane displacements, may be effective in vibronic-spin-orbit coupling with $^1B_{3u}$ ($\sigma\pi^*$ or $n\pi^*$) states via τ_{ii} (A_u). This interaction, however, will be at least an order of magnitude less effective than the direct spin-orbit coupling via τ_i (B_{3u}) which gives rise to sub-spectrum I. From the Raman data, however, assignment for the b_{3g} modes are made. A careful examination of the high resolution phosphorescence spectra in Fig. 5 reveals very weak transitions at the appropriate wavelengths. These are tentatively assigned as b_{3g} vibrations and are indicated in Fig. 5a by the arrows (↑) beneath the spectra. The transitions are too weak to study with PMDR methods without the use of time averaging techniques.

A summary of the spin sublevels responsible for the major and minor routes in the phosphorescence spectra of TBB and TCB is present in Figure 8. The major routes are indicated with a heavy line while the minor routes are indicated with a dashed line. An important feature common to both TBB and TCB is that the τ_z (A_u) spin sublevel which is dipole forbidden to the electronic origin is most strongly spin-orbit coupled to the singlet states. This accounts for the fact that the b_{2g} vibronic origin is more intense than the electronic origin even though vibronic-spin-orbit coupling is expected to be smaller than spin-orbit only.

F. Geometry of the Excited State

The appearance of a progression in a non-totally symmetric vibration, with the maximum intensity in other than the first member, has been taken as evidence of a change of geometry in the excited electronic state.[38] The progression forming vibration is one which transforms as the totally symmetric irreducible representation of the new excited state point group. While this is generally true for transitions between the ground state (assumed to be a singlet) and non-degenerate singlet states observed either in absorption or emission, these conclusions cannot be directly extended to transitions between the ground state and excited triplet states because of the consequences of the triplet state spin degeneracy. The appearance in phosphorescence of an apparent progression in a non-totally symmetric vibration, with the maximum intensity in

either first or second member and a pronounced alternation in the intensity of odd and even members of the progression can arise from different spin sublevels contributing to the even and odd members. This could easily arise for example in a molecule of C_{2v} or D_{2h} symmetry with two spin sublevels differing in total symmetry by the species of a vibration, v. If a transition between one of these spin sublevels, τ_i and the ground state is allowed by electric dipole selection rules, then even quanta of the vibration may appear as totally symmetric harmonics. Transitions from the second spin sublevel, τ_{ii}, may or may not be allowed by electric dipole selection rules, but since $\Gamma_v \times \Gamma_{\tau_{ii}} = \Gamma_{\tau_i}$, vibronically induced components may appear for odd quanta of the non-totally symmetric vibration. Since vibronically induced intensity is, in general, an order of magnitude less intense than electric dipole allowed intensity, one might expect the intensity maximum to remain in the electronic origin, with the even quanta more intense than the odd. If, however, the spin sublevel which gives rise to the vibronically induced intensity (odd members of the progression) has the larger steady state population and the largest total singlet character effective in electric dipole activity to the ground state, then the intensity maximum could appear in the first member of the progression with the odd members more intense than the even.

Several examples of D_{2h} molecules which exhibit this type of unusual progression activity in phosphorescence are provided by 1,4-dibromobenzene,[4] 1,4-dichlorobenzene,[24] and the two tetrahalogenated

molecules discussed in the present paper. Common to the phosphorescence spectra of all these molecules is the presence of a progression in the carbon-halogen, b_{2g} out-of-plane bending mode.[39,40] The progression is most pronounced in 1,4-dibromobenzene[4] where it may be followed through 17 members, with a clear alternation of intensity between the odd and even quanta. The intensity maximum is in the first member of the progression and a satisfactory analysis may be made in terms of two interpenetrating progressions without invoking a change of geometry in the excited state. In the remaining molecules the progression is far less pronounced, numbering only 4 to 6 members. An alternation in intensity is still apparent and the intensity maximum in all cases occurs in the first member of the progression. In each of these compounds, then, it is possible to obtain a satisfactory vibronic analysis assuming an undistorted excited state geometry with at least two active spin sublevels giving rise to two interpenetrating progressions, one of even quanta and one of odd quanta with the Franck-Condon maximum[41] in the first member respectively. The PMDR spectra of TCB and TBB clearly indicate that the odd and even members of this progression originate from different spin sublevels. In the 2|E| PMDR spectrum of TBB, for example, even members of the progression increase in intensity and odd members decrease, indicating different zero-field origins and from the PMDR analysis the even members and odd members originate from the B_{3u} (τ_y) and A_u (τ_z) spin sublevels respectively. Moreover an analysis of the radiative rate constant ratios in TCB (Table V) indicate that the A_u (τ_z) spin sublevel has approximately four times the singlet character of the B_{3u} (τ_y) spin sublevel. This

appears to be sufficient for the b_{2g} vibronic origin to appear more intense than the electronic origin in the 1.3°K phosphorescence spectra.

An interesting feature of the phosphorescence spectra of TBB (neat) at 4.2°K is the disappearance of the 1.3°K trap origin and the appearance of at least three distinct overlapping spectra each having different electronic origins and showing the same b_{2g} progression, but each having the Franck-Condon maximum in a different member. These are illustrated in Fig. 6. The spectra labeled by (**) consist of an electronic origin and an alternating progression of b_{2g} vibrations that can be followed out to eight members. The Franck-Condon maxima of both the even and odd members occur in $0\text{-}2\nu_1$ and $0\text{-}\nu_1$ respectively. The second spectrum is labeled by (o) and consists again of an alternating b_{2g} progression that can be followed out to ten members; however, the Franck-Condon maxima in the even and odd members occur in fourth and fifth members respectively. The third spectrum is labeled by (●) and can be followed out to thirteen members of a b_{2g} progression. In this spectrum alternation is observed only near the Franck-Condon maximum, the eighth for the even members and the ninth for the odd members. Finally other spectra can be seen that have their electronic origin at even lower energy than those above and having Franck-Condon maxima in even higher members. The broad maximum in the phosphorescence intensity around 4200 Å has been taken as evidence for eximer interaction in the triplet state. An interpretation consistent with the above observations is that the three overlapping spectra represent three distinct traps, each being distorted in the excited triplet state. Apparently the deeper the trap the greater is the distortion judging from

relative Franck-Condon maxima in each progression. It is not clear why the 1.3°K origin shows no evidence for distortion unless the nature of trap plays an important role in determining the excited state geometry.

Another unusual feature of the spectra of TCB and TBB is the complete lack of "mirror image" symmetry between the phosphorescence and absorption to that obtained for TCB by George and Morris,[24] and consists principally of an intense electronic origin and several vibronic features whose polarizations are the same as totally symmetric excited state fundamentals. Even though there is a strong vibronic progression in a totally symmetric vibration in absorption, the vibronic origin involving the b_{2g} carbon-halogen out-of-plane bond which is the most prominent feature of the 1.3°K phosphorescence spectrum is scarcely evident in absorption. The lack of "mirror image" symmetry can be in part due to the enhancement of sub-spectrum II relative to sub-spectrum I in phosphorescence if the population in the A_u (τ_z) spin sublevel is sufficiently larger than in the B_{3u} (τ_y) spin sublevel. Since the populations of the individual spin sublevels are a factor in determining the total phosphorescence intensity of a particular vibronic feature, but are not a consideration in the absorption spectrum, this could account in part for the observed differences between emission and absorption. Although it has been demonstrated that sub-spectrum II originates from the A_u (τ_z) spin sublevel which has a larger steady state population than the B_{3u} (τ_y) spin sublevel which is responsible for sub-spectrum I, an explicit analysis of the differences must include differences in the b_{2g} vibrational wavefunctions in the $^3B_{1u}$ state and the vibronically coupled $^3B_{3u}$ state.

G. Interpretation of the Spin Hamiltonian Parameters of TBB and TCB

The structure associated with zero-field electron spin transitions of phosphorescent triplet states can be understood in terms of a spin Hamiltonian which includes the electron spin dipolar interactions in the form of the zero-field Hamiltonian, H_{SS}, the nuclear quadrupole interactions and nuclear-electron hyperfine interactions, H_Q and H_{HF}, respectively.[42]

1. Nuclear quadrupole interactions in the excited $^3\pi\pi^*$ states.

The description of the spin Hamiltonian for molecules with half integral nuclear spin such as chlorine ($I = 3/2$) or bromine ($I = 3/2$) has been treated explicitly by Buckley and Harris for the $^3\pi\pi^*$ state of 8-chloroquinoline[43] and 1,4-dichlorobenzene.[14] The important features of zero-field electron spin resonance measurements in molecules containing nuclei whose spin is greater than 1/2 is that it provides a straightforward method for obtaining excited state field gradients via nuclear quadrupole interactions, H_Q. In short, since H_{SS} and H_Q depend upon the S^2 and I^2 operators, respectively, the nuclear quadrupole splittings appear in zeroth order as satellites split from the major zero-field electron spin transition by the nuclear quadrupole frequency. These satellites correspond to "forbidden" transitions and involve simultaneous changes in the electron and nuclear spin states. The presence of a finite hyperfine interaction at the nucleus is generally sufficient to provide

enough intensity into the satellites via second-order perturbations and under conditions of high microwave power they may be observed. Although the frequencies of these transitions are shifted by H_{HF} in second order the magnitude of the shift for Cl and N hyperfine interactions in $\pi\pi^*$ triplet states are only a few tenths of a MHz and consequently for all practical purposes the separation of the satellites yields the nuclear quadrupole coupling constant directly. In the present investigation, the linewidths of the transitions are too broad for any explicit hyperfine interactions to be determined. It is expected, however, that in the case of ^{35}Cl in TCB, the value of the out-of-plane component, A_{xx}, would be similar to those reported in ^{35}Cl for paradichlorobenzene[14] and 8-chloroquinoline,[43] ~20 MHz. It is difficult to estimate A_{xx} for Br in TBB as no values for triplet states are available.

Values for ^{35}Cl and ^{37}Cl and ^{14}N nuclear quadrupole coupling constants have recently been obtained for molecules in excited triplet states;[6,14,43] however, no quadrupole coupling constants for ^{79}Br and ^{81}Br have heretofore been reported. These can be obtained from an analysis of the zero-field transitions in TBB in Fig. 2, where both the $2|E|$ and $D-|E|$ electron spin transitions are illustrated. In both cases the spectra were obtained monitoring the phosphorescence to the electronic origin at 1.35°K. The maximum microwave power level was ~0.03 gauss. At low power only the electron spin only transitions centered at 6.089 and 7.104 GHz were observed. As the power is increased three sets of "forbidden" satellites split off the major transition appear. The outer pair of satellites are split off the center peak by 277 MHz and 230 MHz respectively and correspond to simultaneous electron-nuclear transition associated with

the ^{79}Br and ^{81}Br respectively. The separation between the outer pairs of satellites are in zeroth order the nuclear quadrupole coupling constants for ^{79}Br and ^{81} Br respectively for TBB in its excited $^3B_{1u}$ state. The inner pair of satellites separated from allowed electron spin transition by only 47 MHz also corresponds to simultaneous nuclear and electron spin transitions; however, as has been described[14] in the case of other halo substituted benzenes, they are associated with only molecules that contain both bromine isotopes. The frequency separation between these satellites is simply the difference between the ^{79}Br and ^{81}Br nuclear quadrupole coupling constants. These values as well as the values obtained from an analysis of the ODMR spectra in TCB both in durene and in neat crystals are listed in Table VI along with the corresponding ground state values. On the average, in the molecules studied to date (except 1,4-dichlorobenzene) the halogens show approximately a 4% reduction in their quadrupole coupling constants in the excited state. Because the triplet states are $\pi\pi^*$ (as opposed to $\sigma\pi^*$) one does not expect an appreciable change in the carbon-halogen sigma bonding; therefore, the reduction in the field gradient presumably occurs either through an increased double bond character in the carbon-halogen bond in the excited state or through σ-π mixing via a small out-of-plane (or in-plane) distortion. Although one cannot distinguish between these possibilities the reduction of the field gradient by a molecular distortion seems unlikely in view of other evidence. The fact that the spin sublevels active in phosphorescence in TBB and TCB can be completely understood in terms of the molecular point group D_{2h} supports the view

that there is no distortion. Specifically, the A_u spin sublevel in TBB and TCB (in durene) is completely inactive to the electronic origin as expected in D_{2h}. In the y-trap of TCB it accounts for ~20% of the dipole activity suggesting a reduction of the symmetry to lower order subgroup of D_{2h}. In spite of this reduction in symmetry, the ^{35}Cl quadrupole coupling constants in neat TCB only differ by 1% from the values in durene. We would like to suggest therefore that the small (4%) reduction in the field gradients in the $\pi\pi^*$ triplet state result from a slight increase in double bond character.

2. The zero-field splittings.

The absolute signs of the zero-field parameters cannot be easily determined experimentally; however, there are good reasons for believing that, like most $\pi\pi^*$ states of aromatic molecules, the TCB value for D is positive. In addition a positive value for E is expected with tetra-substitution in a $^3B_{1u}$ state.[12] It has been shown that the spin sublevels are ordered $\tau_z > \tau_y \gg \tau_x$ (or $\tau_x \gg \tau_y > \tau_z$) in TCB and that these states have spin-orbit symmetries A_u, B_{3u}, and B_{2u} respectively, corresponding to a $^3B_{1u}$ orbital excited state. In the absence of spin-orbit coupling contributions to the zero-field splittings the effects on the zero-field parameters from chlorine substitution to benzene can be qualitatively understood from a molecular orbital approach. The highest occupied molecular orbital in benzene has e_{1g} symmetry. In the point group D_{2h} this reduces to b_{2g} and b_{1g}. Simple first-order perturbation theory requires that 1,2,4,5 halogen substitution will

result in a splitting such that the b_{1g} orbital lies above the b_{2g}. Since the lowest unoccupied molecular orbital in benzene is e_{2u} and in D_{2h}(TCB) this correlates with b_{3u} and a_u, it is expected that the $^3B_{1u}$ state will be derived from the one-electron molecular orbitals b_{1g} and a_u. These molecular orbitals have a nodal plane through the positions 3 and 6; consequently, the spin density from the unpaired electrons in b_{1g} and a_u is located principally on carbons 1, 2, 4 and 5. This is illustrated in Fig. 9 in the coordinate system adopted. The net result of this spin distribution is to produce a large spin dipolar repulsion between the unpaired electrons along the z direction from carbon 1:2 and 4:5 interactions; consequently $\tau_z > \tau_y$. By analogy to benzene and from other studies of aromatic molecules in $\pi\pi^*$ triplet states,[33] the principal axis of the zero-field tensor is along x and τ_x is the lowest spin sublevel. This simple picture is consistent with the magnitude of the zero-field parameter E and all of the PMDR data. A more detailed description of the relationship of the zero-field parameters and the orbital symmetry of substituted benzenes has been given by Buckley, Harris and Panos.[12]

The zero-field parameters of TBB are not so easily understood as those of TCB. Several anomalies need to be explained. First, the values for both D and E represent the largest zero-field splittings known for planar aromatic $^3\pi\pi^*$ states and second, the relative signs of D and E are different than are found in TCB. As in TCB, considering only the spin-dipolar contributions to the zero-field splitting, one expects a positive D value and a positive E. TBB, however, must have relative signs $\pm D \mp E$

in order to explain the PMDR data. This means either $\tau_y > \tau_z > \tau_x$ (+D,-E) or $\tau_x > \tau_z > \tau_y$ (-D,+E). The very large D value in TBB we believe reflects a substantial contribution of spin-orbit coupling to the zero-field parameters. It has been demonstrated that τ_z and τ_y contain most of the dipole activity and therefore have the largest singlet admixtures. If we suppose that the spin-orbit perturbation is principally associated with τ_z and τ_y as has been demonstrated, it seems possible that a large perturbation could depress the τ_z and τ_y spin sublevels below the τ_x spin sublevel; consequently, the sign of D is reversed. Given the D value for TCB as +0.15 cm^{-1} and for TBB as -0.32 cm^{-1}, the increased spin-orbit contributions to D from bromine substitution (vs. chlorine) would be 0.47 cm^{-1}. This value is at least qualitatively consistent with the lifetimes of the spin states τ_y (1.2 ms) and τ_z (0.9 ms) which strongly spin-orbut coupled to singlets and the large oscillator strength (10^{-7}- 10^{-8}) of the $T_1 \leftarrow S_o$ transition.

V. SUMMARY

ODMR and PMDR studies reported for TBB which show that the orbital symmetry is $^3B_{1u}$ and that the spin sublevels are ordered either as $\tau_x > \tau_z > \tau_y$ or $\tau_y > \tau_z > \tau_x$. The large zero-field values suggest that spin-orbit coupling contributions to the zero-field values are significant and are in accord with former spin sublevel order. The major route for phosphorescence to the electronic origin and all totally symmetric vibrations has been shown to be from the τ_y (B_{3u}) spin sublevel while the b_{1g} and b_{2g} vibronic routes result principally from τ_z (A_u). There is no evidence either from the PMDR or excited state ^{79}Br and ^{81}Br nuclear quadrupole coupling constants for a distortion of TBB in its triplet state to a point group lower than D_{2h}. The lifetimes of the τ_y and τ_z spin sublevels were shown to be substantially shorter than τ_x.

The general results from the ODMR and PMDR studies on TCB are essentially the same as in TBB with the exception that the zero-field parameters can be explained without involving spin-orbit coupling contributions: the spin sublevels are shown to be ordered $\tau_z > \tau_y > \tau_x$, consistent with simple orbital arguments. As in TBB no evidence can be found for a distorted excited state.

Finally, the appearance of a progression in the non-totally symmetric b_{2g} vibrations in the halogenated benzenes with the maximum intensity in other than the first member is explained in terms of the radiative rates and populations in the individual spin sublevels with a change in the excited electronic state geometry.

Table I. Vibronic Analysis of the Phosphorescence Spectrum of 1,2,4,5-tetrabromobenzene (1%) in Durene at 1.35°K

Frequency (cm^{-1})	Difference (cm^{-1})	Intensity	PMDR Code	Assignment
26,452	0-0	24/5	+-+/+-+	0-0 electronic origin
26,244	208	73/29	++-/+++	0-208 b_{2g} fundamental
26,127	325	13/23	+++/o+-	0-325 b_{1g} fundamental
26,035	417	4/2	o-+/ooo	0-2 x 208 a_g
25,829	623	11/4	o+-/+++	0-3 x 208 b_{2g}
25,807	645	2/1	ooo/ooo	0-2 x 325 a_g
25,782	670	4/2	o-+/ooo	0-670 a_g fundamental
25,755	677	8/4	++o/+++	0-677 b_{2g} fundamental
25,601	851	7/2	o+-/+++	0-208-2x325 b_{2g}
25,584	868	10/3	o+-/+++	0-868 b_{2g} fundamental
25,573	879	20/7	o+-/+++	0-208-670 b_{2g}
25,457	995	2/3	+o+/o+-	0-325-670 b_{1g}
25,326	1126	11/2	+-+/+-+	0-1126 a_g fundamental
25,299	1153	6/1	+-+/o-+	0-1153 a_g binary
25,118	1334	27/10	++-/+++	0-208-1126 b_{2g}
25,090	1362	16/5	++-/+++	0-208-1153 b_{2g}
25,005	1447	6/9	+++/o+-	0-325-1126 b_{1g}
24,976	1476	3/5	+++/o+-	0-325-1153 b_{1g}
24,925	1527	10/2	--+/--o	0-1527 (?)
24,905	1547	12/4	o+-/+o+	0-208-2 x670 b_{2g}
24,889	1563	7/3	o+-/ooo	0-1563 b_{2g} combination
24,716	1736	26/13	++-/+++	0-208-1527 b_{2g}

Table II. Zero-Field Microwave Transition Frequencies for 1,2,4,5-tetrabromobenzene and 1,2,4,5-tetrachlorobenzene.

Zero-Field Microwave Transition	TBB (neat)	TBB(durene)	TCB (neat: y-trap)	TCB(durene)
D+|E|	11,876.0	13,190	5439.8	5427
D-|E|	7422.5	7104	3612.8	3681.7
2|E|	4437.7	6086	1829.1	1745.3

All frequencies are in MHz

Table III. Vibronic Analysis of the Singlet-Triplet Absorption Spectrum of 1,2,4,5-tetrabromobenzene at 1.35°K.

Frequency (cm^{-1})	Intensity	Difference	Analysis
26,734	vvs	0-0	electronic origin
26,739	vs	5	lattice fundamental
26,743	vs	9	2 x 5 lattice
26,756	vvs	22	lattice fundamental
26,882	w	148	
26,954	m	220	
27,237	s	503	
27,274	vvs	540	540 a_g fundamental
27,367	m	633	
27,407	w	673	
27,563	s	831	
27,824	vs	1090	2 x 540 = 1080
28,381	vs	1647	3 x 540 = 1620
28,653	m	1919	
28,921	s	2187	4 x 540 = 2170

Table IV. Vibrational Analysis of the Raman Spectrum of Crystalline 1,2,4,5-tetrabromobenzene.

Frequency (cm^{-1})	Intensity	Assignment	Method
130	100+	a_g fundamental	Raman
208	26	b_{2g} fundamental	Raman-PMDR
211	25	b_{3g} fundamental	Raman
224	83	a_g fundamental	Raman
322	38	b_{1g} fundamental	Raman-PMDR
410	..	2 x 208 (b_{2g}) = 416 a_g	Raman-PMDR
459	29	2 x 224 (a_g) = 448 a_g or b_{3g} fundamental	Raman
661	39	a_g fundamental	Raman-PMDR
672	73	b_{2g} fundamental	Raman-PMDR
806	14	b_{3g} fundamental	Raman
870	13	b_{2g} fundamental	Raman-PMDR
1125	75	a_g fundamental	Raman-PMDR
1150	40	672 (b_{2g}) + 459 (b_{3g}) = 1131 b_{1g}	Raman
1250	18	130 (a_g) + 1125 (a_g) = 1255 a_g or b_{3g} fundamental	Raman
1345	22	208 (b_{2g}) + 1125 (a_g) = 1333 b_{2g}	Raman-PMDR
1529	35	a_g fundamental	Raman-PMDR
1543	68	b_{3g} fundamental	Raman

Table V. Summary of the ODMR and PMDR Results for 1,2,4,5-tetrabromobenzene and 1,2,4,5-tetrachlorobenzene.

	TBB (in durene) (cm^{-1})	TBB (neat) (cm^{-1})	TCB (in durene) (cm^{-1})	TCB (single crystal y-trap) (cm^{-1})
a_g (Electronic origin)	26,452	26,699	26,444*	26,626
b_{1g} origin	(-325)	(-333)	(-351)	(-363)
b_{2g} origin	(-208)	(-209)	(-234)*	(-233)
D+|E| PMDR (relative intensity)				
a_g	See Figure 3	+15	0	+2
b_{1g}	"	+2	0	+3
b_{2g}	"	+5	0	+15
D-|E| PMDR (relative intensity)				
a_g (origin)	See Figure 4	-9	+8	+12
b_{1g}	"	+2	0	+3
b_{2g}	"	+9	0	+15
2|E| PMDR (relative intensity)				
a_g	See Figure 5	-2.5	+10**	-19
b_{1g}	"	0	+1**	+3
b_{2g}	"	+1	-7**	+15
Total decay (1/e)				
τ_x	13 ± 1 ms	--	~ 700 ms*	860 ± 15 ms
τ_y	1.22 ± .05 ms	--	33 ms*	28 ± 1 ms
τ_z	0.95 ± .05 ms	--	37 ms*	22 ± 1 ms
Relative Radiative Rate Constants				
τ_x (a_g)	< 0.1	--	--	< 0.1
τ_y (a_g)	2	--	--	5
τ_z (a_g)	0	--	--	1
τ_x (b_{2g})	< 0.1	--	--	< 0.1
τ_y (b_{2g})	0	--	--	1
τ_z (b_{2g})	5	--	--	3

* Data from Reference 25.
** Data essentially the same as in Reference 25.

Table VI. Nuclear Quadrupole Coupling Constants

	Excited Triplet State	Ground State	Nucleus
TBB (Neat)	280 ± 7 MHz	288 MHz*	^{79}Br
TBB (in Durene)	277 ± 2 MHz		^{79}Br
TCB (Neat)	34.8 ± 0.5 MHz	36.7 MHz**	^{35}Cl
TCB (in Durene)	35.2 ± 0.5 MHz		^{35}Cl

* From Reference 44.

** From Reference 45.

REFERENCES

1. H. Shull, J. Chem. Phys. 17, 295 (1949); D. S. McClure, J. Chem. Phys. 17, 665 (1949); D. P. Craig, J. Chem. Phys. 18, 236 (1950).

2. M. Goeppert-Mayer and A. L. Sklar, J. Chem. Phys. 6, 645 (1938); C. C. J. Roothaan and R. S. Mulliken, J. Chem. Phys. 16, 118 (1948); C. C. J. Roothaan and R. G. Paar, J.Chem. Phys. 17, 1001 (1949); R. G. Parr, D. P. Craig, and I. G. Ross, J. Chem. Phys. 18, 1561 (1950); K. J. Niira, J. Chem. Phys., 20, 1498 (1952); J. Phys. Soc. Japan, 8, 630 (1953); J. A. Pople, Proc. Phys. Soc. (London) A68, 81 (1955); R. Pariser, J. Chem. Phys. 24, 250 (1956); N. S. Ham and K. Ruedenberg, J. Chem. Phys. 25, 1 (1956); D. R. Kearns, J. Chem. Phys. 36, 1608 (1962); J. R. Platt, J. Mol. Spectroscopy 9, 288 (1962); J. W. Moskowitz and M. P. Barnett, J. Chem. Phys. 39, 1557 (1963); J. M. Schulman and J. W. Moscowitz, J. Chem. Phys. 43, 3287 (1965).

3. O. Schnepp, J. Chem. Phys. 30, 863 (1959); O. Schnepp and R. Kopelman, J. Chem. Phys. 30, 868 (1959); D. W. Olds, J. Chem. Phys. 35, 2248 (1961); G. Castro and R. M. Hochstrasser, Molecular Crystals 1, 139 (1966); G. Castro and R. M. Hochstrasser, J. Chem. Phys. 44, 412 (1966); G. A. George and G. C. Morris, J. Chem. Phys. 54, 815 (1971); R. M. Hochstrasser, J. E. Wessel, J. D. Whiteman and A. H. Zewail, Chem. Phys. Letters 10, 452 (1971).

4. G. Castro and R. M. Hochstrasser, J. Chem. Phys. 46, 3617 (1967).

5. A. C. Albrecht, J. Chem. Phys. 33, 156 (1960); 33, 169 (1960); 38, 354 (1962).

6. M. Sharnoff, J. Chem. Phys. 46, 3263 (1967); A. L. Kwiram, Chem. Phys. Letters 1, 272 (1967); J. Schmidt, I. A. M. Hesselmann, M.S. de Groot and J. H. van der Waals, Chem. Phys. Letters 1, 434 (1967); M. Sharnoff, Chem. Phys. Letters 2, 498 (1968); J. Schmidt and J. H. van der Waals, Chem. Phys. Letters 2, 640 (1968); 3, 546 (1969); I. Y. Chan, J. Schmidt and J. H. van der Waals, Chem. Phys. Letters 4, 269 (1969); C. B. Harris, D. S. Tinti, M. A. El-Sayed and A. H. Maki, Chem. Phys. Letters 4, 409 (1969); M. J. Buckley, C. B. Harris and A. H. Maki, Chem. Phys. Letters 4, 591 (1970); M. A. El-Sayed, D. S. Tinti and D. Owens, Chem. Phys. Letters 3, 339 (1969); M. A. El-Sayed, J. Chem. Phys. 52, 6432 (1970); R. F.Clements and M. Sharnoff, Chem. Phys. Letters 7, 4 (1970); M. A. El-Sayed, J. Chem. Phys. 52, 6432 (1970); M. D. Fayer, C. B. Harris and D. A. Yuen, J. Chem. Phys. 53, 4719 (1970); J. Schmidt, V. C. van Dorp and J. H. van der Waals, Chem. Phys. Letters 8, 345 (1971); A. H. Francis and C. B. Harris, Chem. Phys. Letters 9, 181 (1971).

7. J. Schmidt, W. S. Veeman and H. J. van der Waals, Chem. Phys. Letters 4, 341 (1969).

8. D. S. Tinti and M. A. El-Sayed, J. Chem. Phys. 54, 2529 (1971).

9. C. B. Harris, J. Chem. Phys. 54, 972 (1971).

10. J. Schmidt, D. A. Antheunis and J. H. van der Waals, Molecular Phys. 22, 1 (1971); D. M. Burland and J. Schmidt, Molecular Phys. 22, 19 (1971).

11. C. B. Harris and R. J. Hoover, Chem. Phys. Letters 12, 75 (1971).

12. M. J. Buckley, C. B. Harris and R. M. Panos, J. Am. Chem. Soc. xx, xxxx (1972).

13. M.Schwoerer and H. Sixl, Chem. Phys. Letters 2, 14 (1968).

14. M. J. Buckley and C. B. Harris, J. Chem. Phys. 56, 137 (1972).

15. D. S. Tinti, M. A. El-Sayed, A. H. Maki and C. B. Harris, Chem. Phys. Letters 3, 343 (1969)

16. C. Dean, M. Pollak, B. M.Craven, G. A. Jeffrey, Acta Cryst. 11, 710 (1958).

17. A. Monfils, C. R. Acad. Sci. Paris, 241, 561 (1955).

18. G. Gafner and F. H. Herbstein, Acta Cryst. 13, 702, 706 (1960).

19. F. H. Herbstein, Acta Cryst. 18, 997 (1965).

20. G. Gafner and F. H. Herbstein, Acta Cryst. 17, 982 (1964).

21. M. A. El-Sayed, J. Chem. Phys. 54, 680 (1971).

22. C. B. Harris and R. J. Hoover, J. Chem. Phys. 56, xxx (1972).

23. A. H. Francis and C. B. Harris, Chem. Phys. Letters 9, 188 (1971).

24. G. A. George and G. C. Morris, Molecular Crystals and Liquid Crystals 11, 61 (1970).

25. C. R. Chen and M. A. El-Sayed, Chem. Phys. Letters 10, 307 (1971).

26. The signal-to-noise ratio of the PMDR's of TCB and neat TBB are somewhat less than those illustrated for TBB in durene.

27. R. S. Mulliken, J. Chem. Phys. 23, 1997 (1955).

28. J. M. Robertson, Proc. Roy. Soc. A141, 594 (1933).

29. D. S. McClure, J. Chem. Phys. 17, 905 (1949); 17, 665 (1949); M. Kasha, J. Chem. Phys. 20, 71 (1952).

30. "Electron Spin Relaxation Phenomena in Solids" K. J. Standley and R. A. Vaughan, Adam Hilger Ltd., London, 1969.

31. A. H. Francis and C. B. Harris, J. Chem. Phys. 55, 3595 (1971).

32. The PMDR code in Table V for all molecules and optical transitions are ordered for D+|E|, D-|E| and 2|E| microwave transitions respectively.

33. M. S. de Groot, I. A. M. Hesselmann and J. H. van der Waals, Mol. Phys. 16, 45 (1969); M. Godfrey, C. W. Kern and M. Karplus, J. Chem. Phys. 44, 4459 (1966); M. Gouterman and W. Moffitt, J. Chem. Phys. 30, 1107 (1959); M. Gouterman, J.Chem. Phys. 30, 1369 (1959); B. Smaller, J. Chem. Phys. 37, 1579 (1962); H. Hameka, J. Chem. Phys. 31, 315 (1959); Y. N. Chin, J. Chem. Phys. 39, 2736 (1963); C. A. Hutchison, Jr. and B. W. Magnum, J. Chem. Phys. 34, 908 (1961); N. Hirota, C. A. Hutchison, Jr., and P. Palmer, J. Chem. Phys. 40, 3717 (1964).

34. M. A. El-Sayed and O. F. Kalman, J. Chem. Phys. 52, 4903 (1970).

35. Since one generally sweeps frequency in zero-field ODMR, it is possible to support different mode patterns in different regions of the spectra causing in some cases wide variations in intensity and polarization.

36. M. A. El-Sayed, T. Pavlopoulos, J. Chem. Phys. 39, 1899 (1963); M. A. El-Sayed, J. Chem. Phys. 43, 2864 (1965) and references contained therein.

37. D. S. McClure, J. Chem. Phys. 17, 665 (1949); 20, 682 (1952).

38. R. M. Hochstrasser, J. Chem. Phys. 46, 3617 (1967).

39. J. R. Scherer and J. C. Evans, Spectrochim. Acta 19, 1739 (1963).

40. A. Stojiljkovoic and D. H. Whiffen, Spectrochim. Acta 12, 47 (1951).

41. J. Franck, Trans. Faraday Soc. 21, 536 (1925); E. U. Condon, Phys. Rev. 28, 1182 (1926).

42. J. Schmidt and J. H. van der Waals, Chem. Phys. Letters 3, 546 (1969); C. B. Harris, D. S. Tinti, M. A. El-Sayed and A. H. Maki, Chem. Phys. Letters 4, 409 (1969); M. J. Buckley, C. B. Harris and A. H. Maki, Chem. Phys. Letters 4, 591 (1970).

43. M. J. Buckley and C. B. Harris, Chem. Phys. Letters 5, 205 (1970).

44. P. Bray, J. Chem. Phys. 22, 2023 (1954).

45. P. Bray, J. Chem. Phys. 23, 220 (1955); A. Monfils, Compt. Rend. 241, 561 (1955).

FIGURE CAPTIONS

Figure 1 1.35°K phosphorescence spectra of 1,2,4,5-tetrabromobenzene in durene: arrows below spectrum(a) indicate tentative b_{3g} vibrational assignments.

(a) unpolarized

(b) polarized parallel to the durene a axis

(c) polarized parallel to the durene c' axis

Figure 2 Zero-field optically detected magnetic resonance spectra of 1,2,4,5-tetrabromobenzene at 1.35°K obtained monitoring the electronic origin phosphorescence.

(a) 2|E| microwave transition centered around 6086 MHz

(b) D-|E| microwave transition centered around 7104 MHz

Figure 3 The D+|E| PMDR spectra of 1,2,4,5-tetrabromobenzene in durene at 1.35°K.

(a) unpolarized

(b) polarized parallel to the durene a axis

(c) polarized parallel to the durene c' axis

Figure 4 The D-|E| PMDR spectra of 1,2,4,5-tetrabromobenzene in durene at 1.35°K.

(a) unpolarized

(b) polarized parallel to the durene a axis

(c) polarized parallel to the durene c' axis

Figure 5 The 2|E| PMDR spectra of 1,2,4,5-tetrabromobenzene in durene at 1.35°K.

(a) unpolarized

(b) polarized parallel to the durene a axis

(c) polarized parallel to the durene c' axis

Figure 6 The 4.2°K phosphorescence spectrum of neat 1,2,4,5-tetrabromobenzene.

Figure 7 The 1.35°K polarized $T_1 \leftarrow S_o$ absorption spectra of 1,2,4,5-tetrabromobenzene.

(a) and (b) polarized parallel to c'

(c) polarized parallel to a

Figure 8 Primary and secondary radiative routes in phosphorescence from 1,2,4,5-tetrabromobenzene in durene and from the y-trap of 1,2,4,5-tetrachlorobenzene.

Figure 9 The symmetry and spin density distribution in the b_{1g} and a_u one-electron molecular orbitals for 1,2,4,5-tetrahalobenzenes.

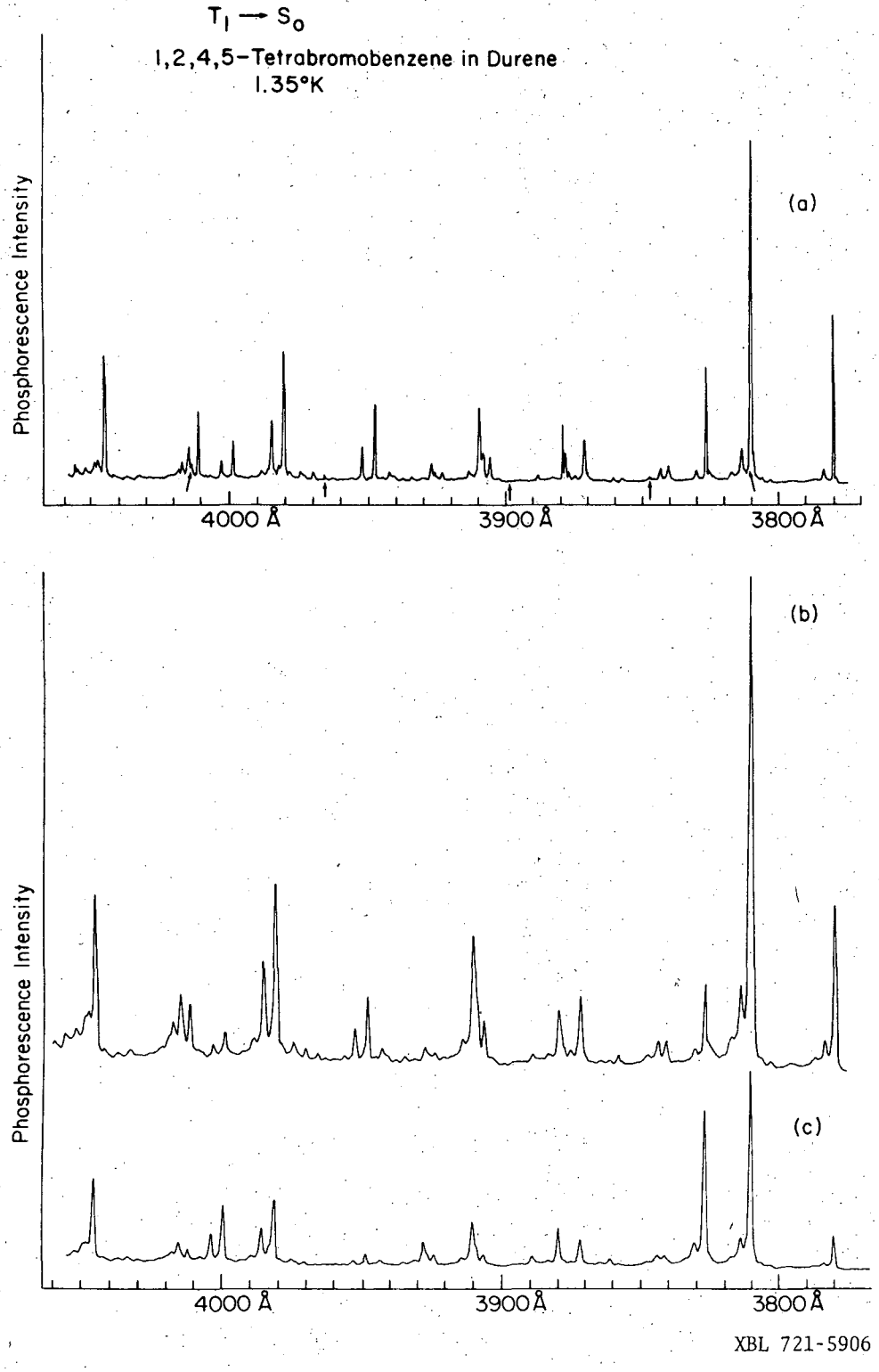
$T_1 \rightarrow S_0$
1,2,4,5-Tetrabromobenzene in Durene
1.35°K
Phosphorescence Intensity
(a)
4000 Å
3900 Å
3800 Å
(b)
(c)
Phosphorescence Intensity
4000 Å
3900 Å
3800 Å
XBL 721-5906

Fig. 1

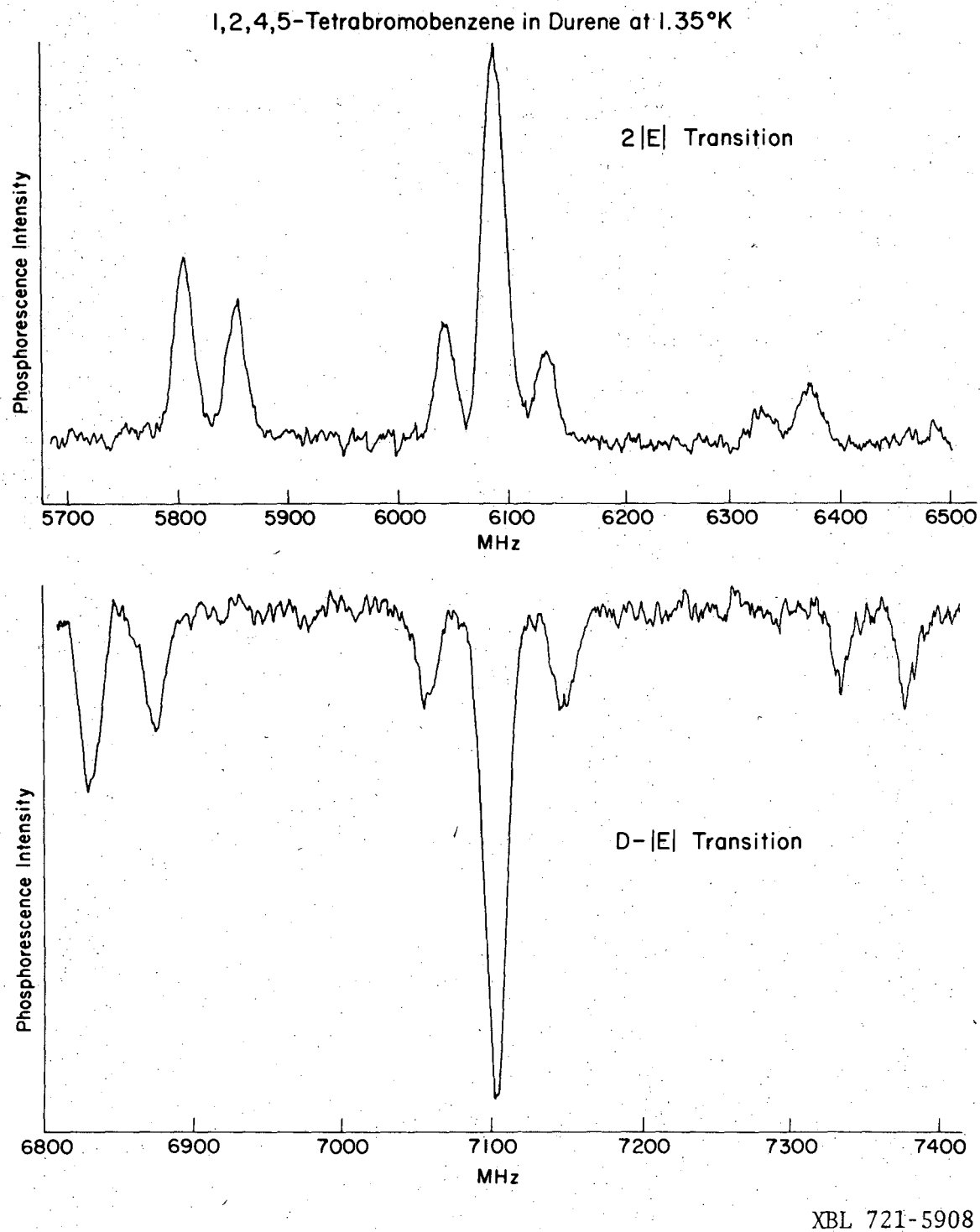
1,2,4,5-Tetrabromobenzene in Durene at 1.35°K
2|E| Transition
Phosphorescence Intensity
5700
5800
5900
6000
6100
6200
6300
6400
6500
MHz
D-|E| Transition
Phosphorescence Intensity
6800
6900
7000
7100
7200
7300
7400
MHz
XBL 721-5908

Fig. 2

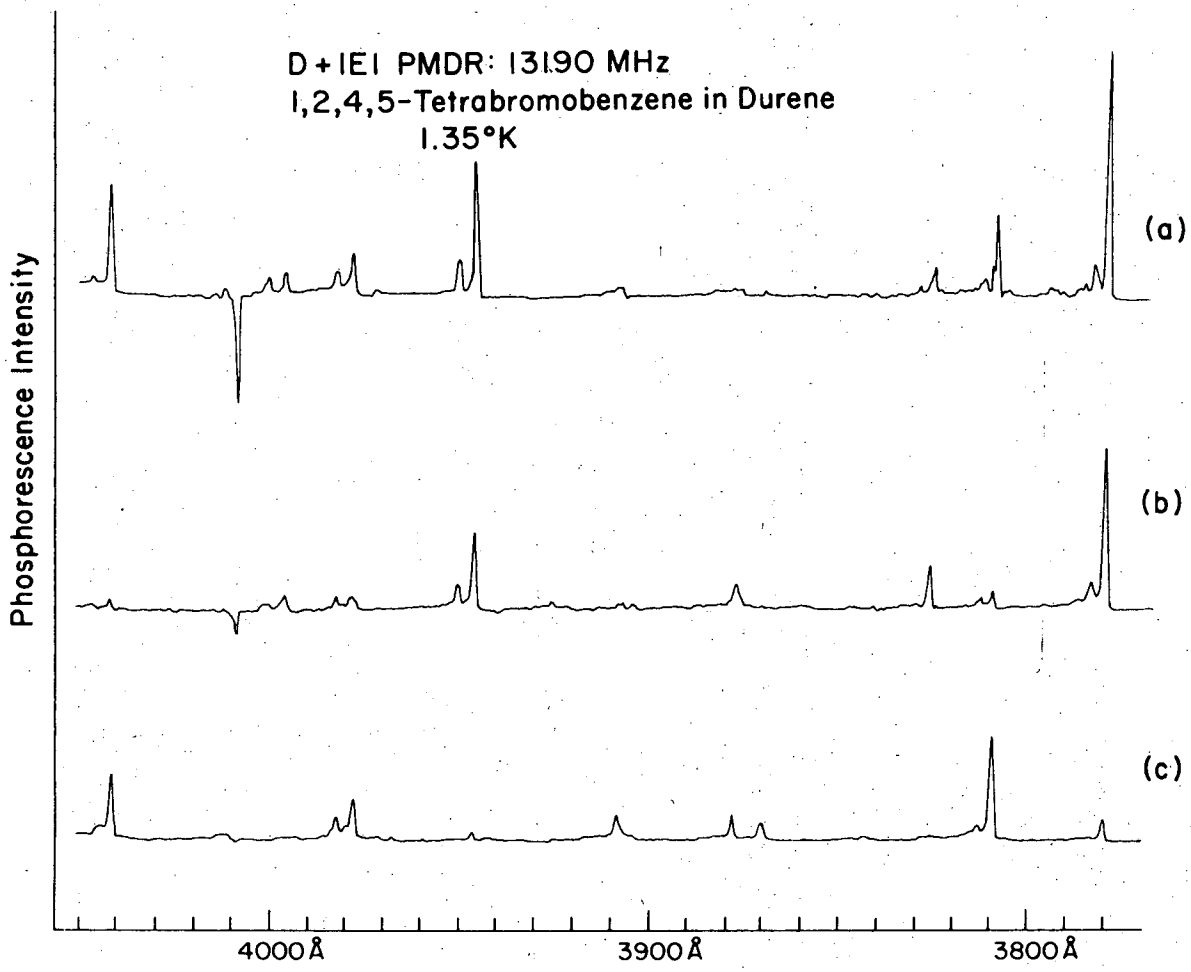

XBL 721-5984

Fig. 3

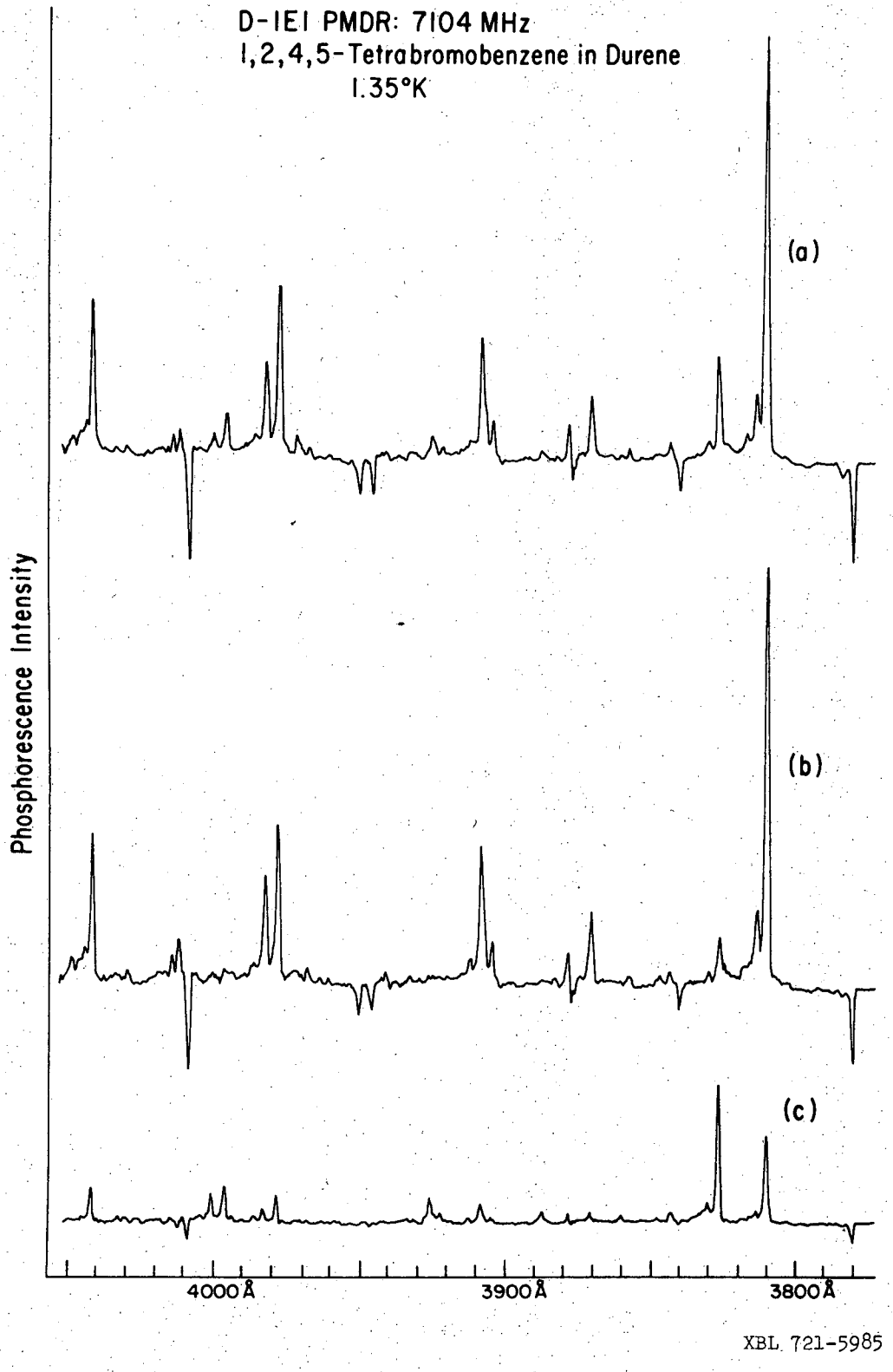
D-IE1 PMDR: 7104 MHz
1,2,4,5-Tetrabromobenzene in Durene
1.35°K
(a)
(b)
(c)
Phosphorescence Intensity
4000Å
3900Å
3800Å
XBL 721-5985

Fig. 4

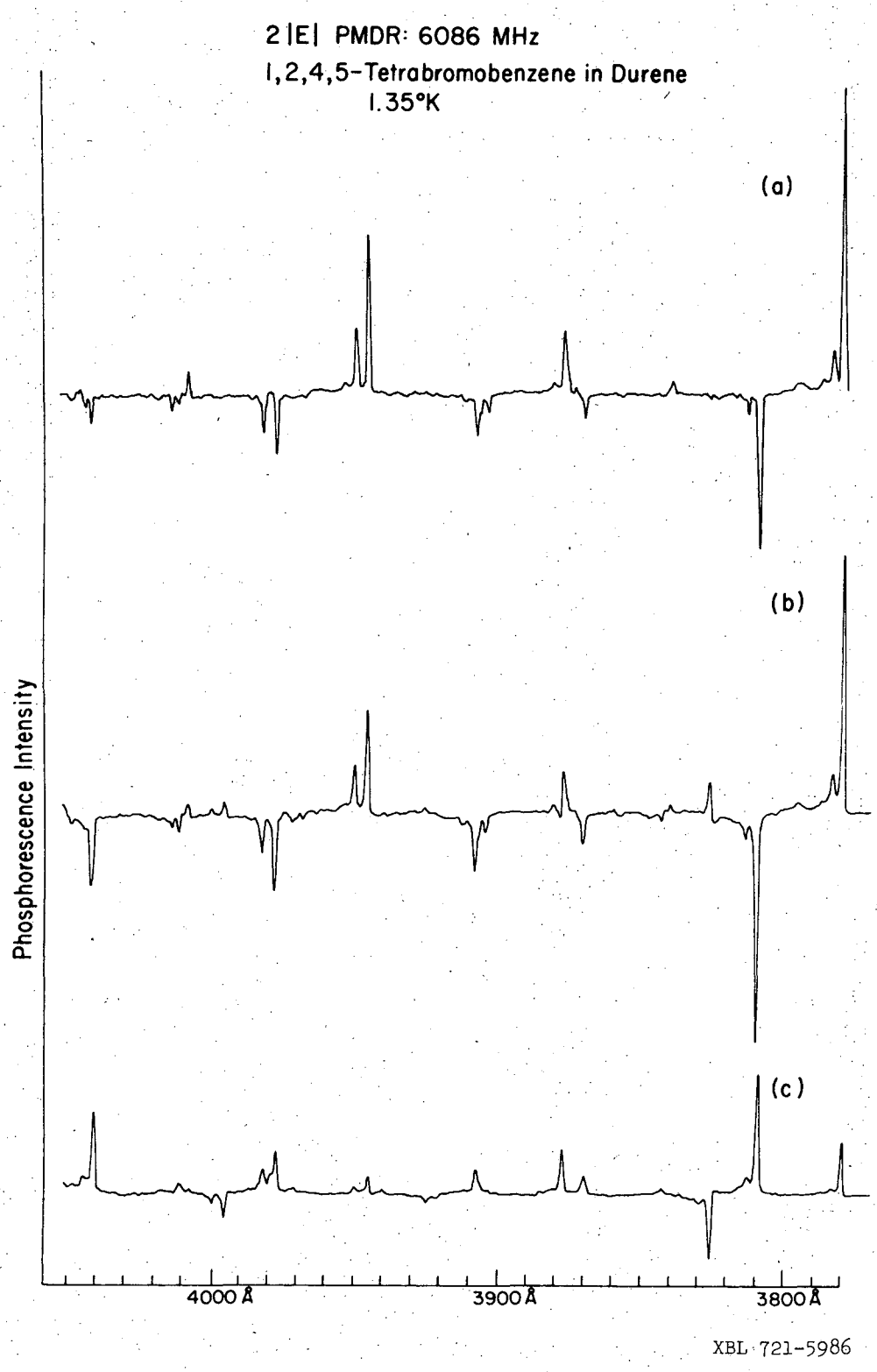
2|E| PMDR: 6086 MHz
1,2,4,5-Tetrabromobenzene in Durene
1.35°K
(a)
(b)
(c)
Phosphorescence Intensity
4000 Å
3900 Å
3800 Å
XBL 721-5986

Fig. 5

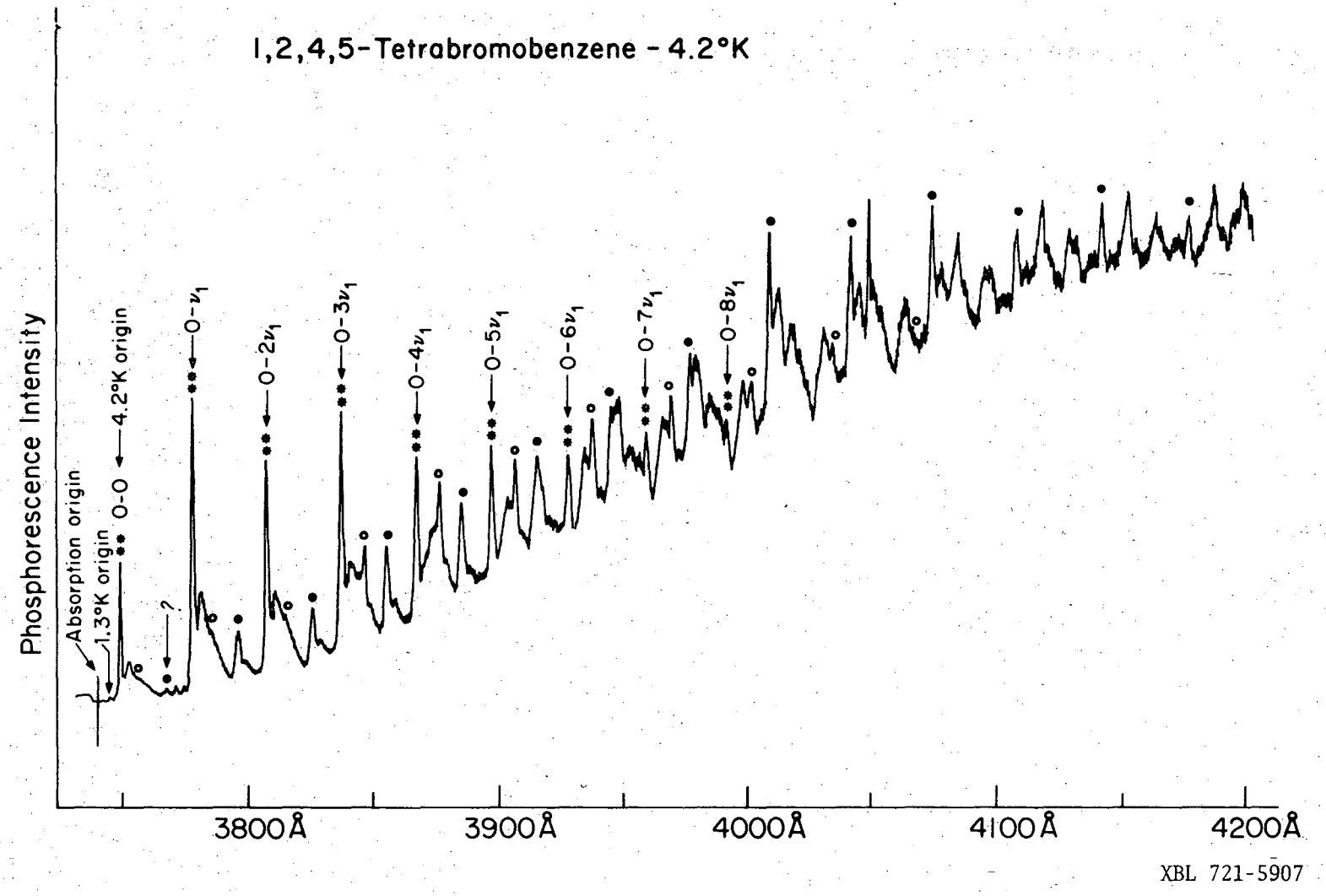
1,2,4,5-Tetrabromobenzene - 4.2°K
Phosphorescence Intensity
Absorption origin
1.3°K origin
** 0-0
4.2°K origin
?
0-ν1
0-2ν1
0-3ν1
0-4ν1
0-5ν1
0-6ν1
0-7ν1
0-8ν1
3800Å
3900Å
4000Å
4100Å
4200Å
XBL 721-5907

Fig. 6

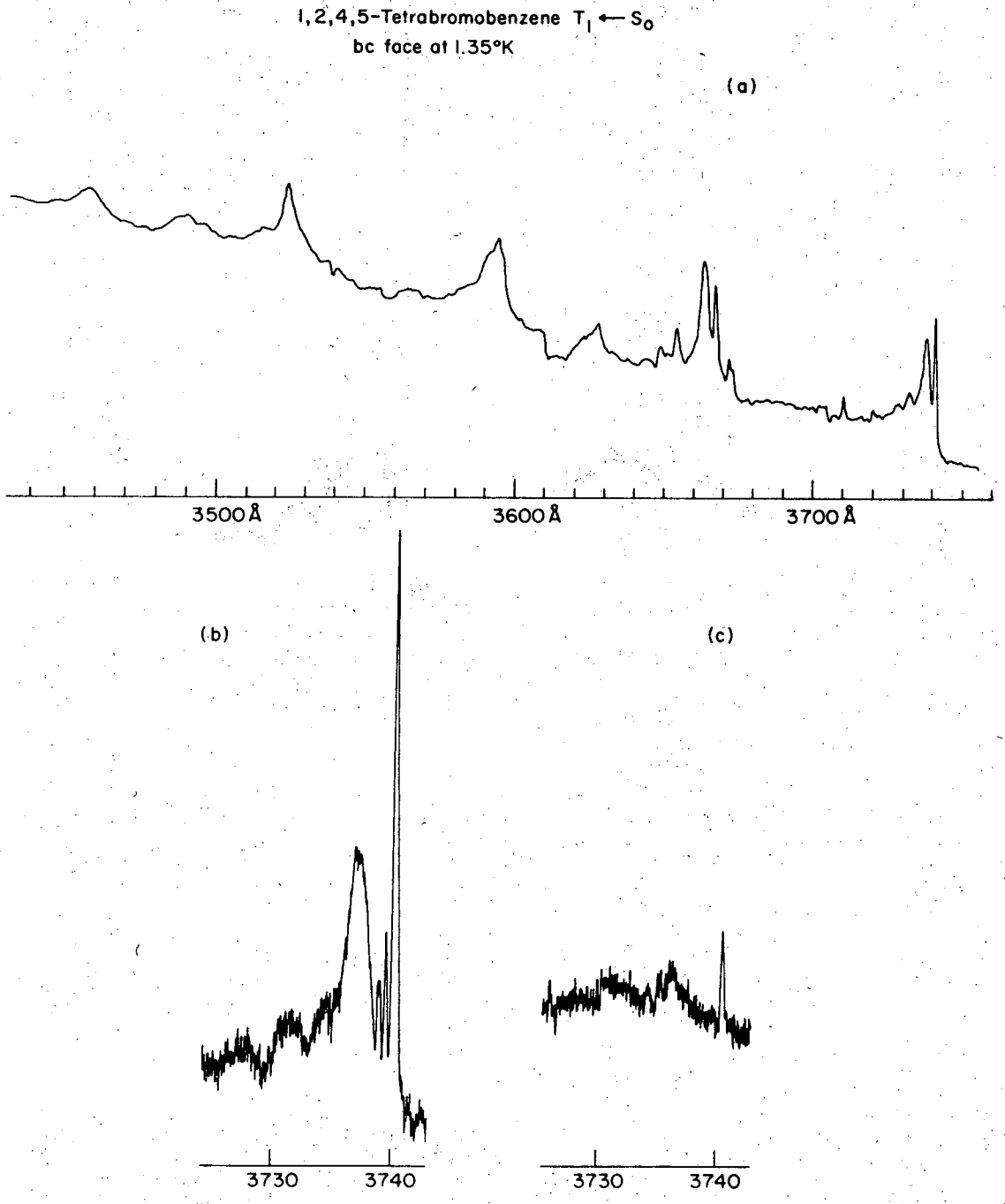
1,2,4,5-Tetrabromobenzene $T_1 \leftarrow S_0$
bc face at 1.35°K
(a)
3500 Å
3600 Å
3700 Å
(b)
(c)
3730
3740
3730
3740
XBL 721-5987

Fig. 7

Primary and secondary radiative routes in 1,2,4,5-tetrabromobenzene and 1,2,4,5-tetrachlorobenzene phosphorescence.

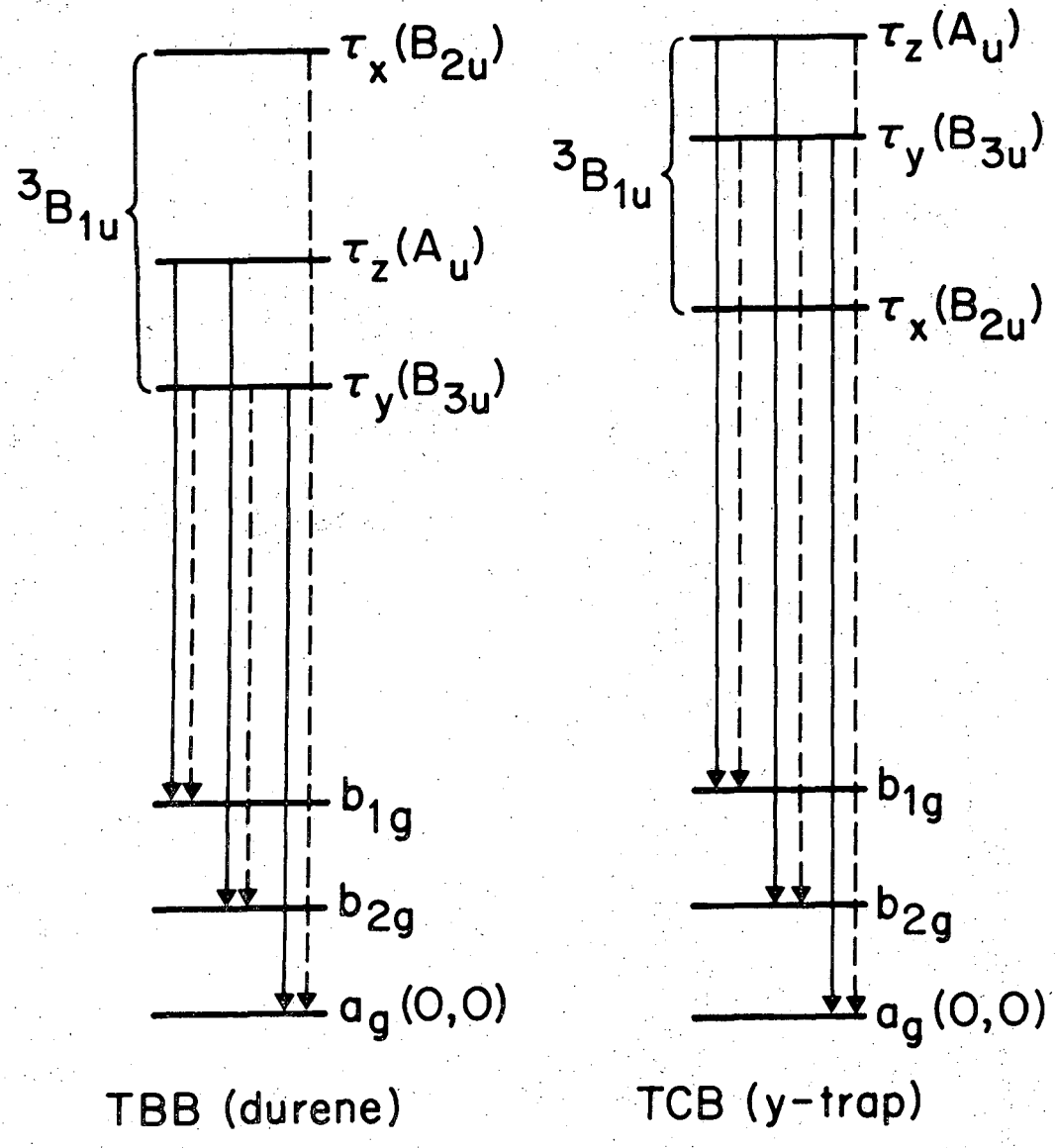

XBL 721-5988

Fig. 8

Symmetry and spin density distribution in 1,2,4,5 tetrachlorobenzene one-electron molecular orbitals.

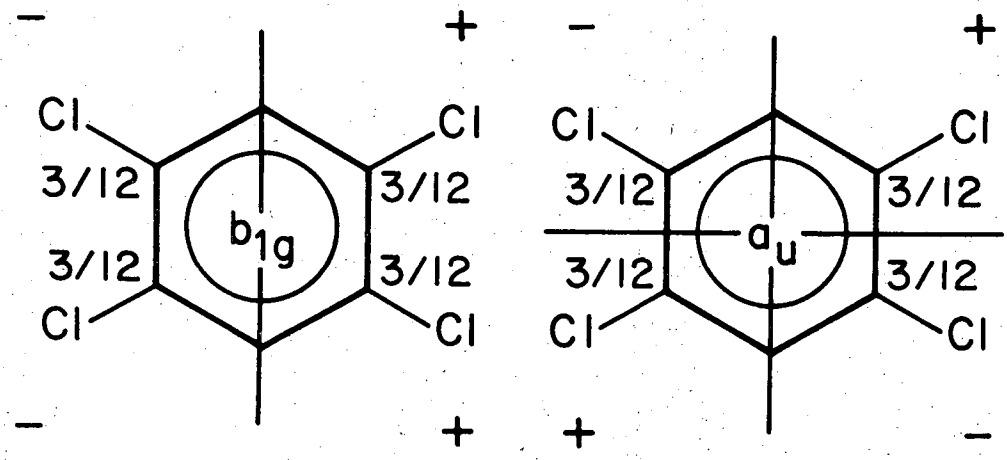

XBL 721-5989

Fig. 9

TECHNICAL INFORMATION DIVISION
LAWRENCE BERKELEY LABORATORY
UNIVERSITY OF CALIFORNIA
BERKELEY, CALIFORNIA 94720